JOM, Vol. 64, No. 9, 2012
DOI: 10.1007/s11837-012-0419-9

Computational Fluid Dynamics Modeling: Application to Transport Phenomena During the Casting Process

LIFENG ZHANG[1,2]

1.—School of Metallurgical and Ecological Engineering, University of Science and Technology Beijing, Beijing 100083, China. 2.—e-mail: zhanglifeng@ustb.edu.cn

INTRODUCTION

Fluid flow during steel casting is very important to steel quality because it affects other important phenomena during mixing, refining, and solidification processes. These phenomena include turbulent flow in the molten steel, the transport of bubbles and inclusions, multiphase flow phenomena, chemical and transport interactions between the steel and the slag, the effect of heat transfer, the transport of solute elements, and segregation. With the high cost of empirical investigation and the increasing power of computer hardware and software, computational fluid dynamics (CFD) is becoming an important tool to understand these fluid flow-related phenomena during steelmaking and casting processes.

FLUID-FLOW AND TURBULENCE MODELS

A typical three-dimensional fluid-flow model solves the continuity equation and Navier–Stokes equations for incompressible Newtonian fluids, which are based on conserving mass (one equation) and momentum (three equations) at every point in a computational domain.[1,2] The solution of these equations, given elsewhere,[3] yields the pressure and velocity components at every point in the domain. At the high flow rates involved in this process, these models must incorporate turbulent fluid flow. Many different turbulence models have been employed by different researchers for fluid flow in the molten steel system, such as one equation turbulence models (turbulent energy k plus a given length-scale)[4]; two-equation turbulence models such as the k-ε model[3,5]; large eddy simulation,[6–10] possibly with a subgrid scale model[11,12]; and direction numerical simulation (DNS).[3] Among these models, direct numerical simulation is the simplest yet most computationally demanding method. DNS uses a fine enough grid (mesh) to capture all of the turbulent eddies and their motion with time. To achieve more computationally efficient results, turbulence is usually modeled on a courser grid using a time-averaged approximation, such as the popular k–ε model,[5] which averages out the effect of turbulence using an increased effective viscosity field, μ_{eff}. This approach requires solving two additional partial differential equations for the transport of turbulent kinetic energy and its dissipation rate.[3] The standard high-Reynolds-number k–ε model generally uses assumed "wall functions" to capture the steep gradients at wall boundaries, in order to achieve reasonable accuracy on a course grid.[5,13,14] Alternatively, the low-Reynolds-number turbulence model treats the boundary layer in a more general way but requires a finer mesh at the walls. Large eddy simulation is an intermediate method between direct numerical simulation and k-ε turbulence models, which uses a turbulence model only at the subgrid scale.[6–10]

TRANSPORT OF THE SECOND-PHASE PARTICLES

Two main approaches have been applied to model the behavior of these second-phase particles in the molten steel: the simple convective-diffusion approach and full trajectory calculations. In the convection–diffusion approach,[15–18] particle (inclusion or bubble) motion due to turbulent transport and diffusion is modeled by solving a solute transport equation, with the addition of a particle terminal rising velocity to the vertical direction, as shown in Eq. 1.

$$\frac{\partial \sigma_{\text{P}}}{\partial t} + u_{\text{ip}} \frac{\partial \sigma_{\text{P}}}{\partial x_{\text{i}}} = \frac{\partial}{\partial x_{\text{i}}} \left(D_{\text{eff}} \frac{\partial \sigma_{\text{P}}}{\partial x_{\text{i}}} \right) \tag{1}$$

where σ_{p} is the particle (inclusion or bubble) volume fraction, u_{i} is the liquid velocity; D_{eff} is the effective diffusion coefficient; u_{ip} is the particle velocity, which equals the liquid velocity, except in the vertical direction, where the terminal rising velocity V_{T} should be added, namely, $u_{\text{ip}} = u_{\text{i}} + V_{\text{T}}$.

(Published online August 25, 2012)

In the full trajectory approach,[19–24] each particle trajectory is calculated by integrating its local velocity, defined by considering the different forces that act on it, such as drag and gravity, as given in Eq. 2.

$$\frac{dv_{Pi}}{dt} = -\frac{3}{4}\frac{C_D v_{Pi}\rho}{d_P \rho_P}|v_{Pi} - u_i| + \frac{(\rho_P - \rho)g}{\rho_P} + C_A\left(\frac{du_i}{dt} - \frac{dv_{Pi}}{dt}\right) \quad (2)$$

where ρ_p and ρ are the particle and liquid densities, v_{pi} is the particle velocity, C_D is the drag coefficient as a function of particle Reynolds number, C_A is a constant, and g is gravity acceleration. The first term on the right of this equation is the drag force, which is always opposite to the motion direction. The second term is the buoyancy force due to gravity, and the third term is the "added mass force."[25] The effects of turbulent fluctuations can be modeled crudely by adding a random velocity fluctuation ($\xi\sqrt{2k/3}$) to the mean fluid phase velocity at each step, where ξ is a random number (chosen between 0 and 1 at each increment) and k is the local turbulent kinetic energy.

MULTIPHASE FLUID-FLOW MODELS

The multiphase phenomena in steelmaking include argon injection during steel refining and continuous casting, the entrainment and emulsification of slag at the top of the molten steel, and air/slag/steel interactions during ingot teeming. There are several models to simulate multiphase fluid flow. The algebraic slip model[16,19,26–30] approximates the dispersed two-phase system as a single-phase mixture of liquid and gas. Flow of the liquid–gas mixture is calculated by solving only one continuity equation, one set of momentum equations, and one set of turbulence equations. The gas fraction is calculated from one additional transport equation for the gas phase (Eq. 1). The slip velocity of the argon bubbles depends on their size and shape. Usually, their terminal velocity is used.[18] The buoyancy effect of the gas bubbles on the fluid flow is taken into account by adding an extra force term to the vertical momentum equation: $S_{gz} = -\sigma_g g\rho$, where σ_g is the gas volume fraction. In the Langrangian multiphase model,[31] only one velocity field is solved (i.e., the Eularian liquid velocity), but the liquid volume fraction is included in every term. The liquid volume fraction is calculated from the gas volume fraction, which is solved using the particle trajectory (Eq. 2). This model has been used to calculate two-phase fluid flow in a continuous-casting mold.[32] In the Eularian–Eularian two-phase model approach, velocity fields of each phase are solved, and the total volume fraction of all phases is unit.[20,25,33–35] Bubble-induced turbulence may be added to the k and ε equations through source terms.[25,36] In the volume of fluid (VOF) method,[37] the movement of a free surface is tracked through the computational grid by simultaneously solving the volume of fluid per unit volume (f_i). This requires satisfaction of an additional conservation equation, such as

$$\frac{\partial f_i}{\partial t} + \left[\frac{\partial}{\partial x_i}(f_i u_i)\right] = 0 \quad (3)$$

This method is popular in the simulation of free surface phenomena.[23,24,38]

HEAT-TRANSFER-RELATED PHENOMENA

Fluid-flow models can be extended to predict the variations and evolution of the fluid temperature by solving an additional equation for the transport and dissipation of superheat in the liquid metal. Superheat is the energy contained in the liquid metal above its equilibrium solidification temperature or liquidus temperature. The conservation equation of the thermal energy has been coupled to the flow equations, incorporating Boussinesque's term ($\rho g\beta\Delta T$) into the vertical direction momentum balance equation, where ρ is the density of the molten steel, g is the gravitational acceleration, β is the thermal expansion coefficient, and ΔT is the temperature difference.

SIMULATION OF ELECTROMAGNETIC FORCES ON THE FLUID FLOW IN METALLURGICAL SYSTEMS

The application of magnetohydrodynamics to control the flow of molten steel started with electromagnetic stirring (EMS) of the strand pool with a traveling (alternating) magnetic field. It has now advanced to electromagnetic stirring in the mold and to an in-mold direct-current magnetic field, which induces a braking force to slow the flow (EMBr) in the continuous caster. Owing to the difficulty of conducting measurements, development of EMS and EMBr must rely heavily on computational modeling. The flow pattern and mixing under the application of electromagnetic forces can be modeled by solving the Maxwell, Ohm, and charge conservation equations for electromagnetic forces simultaneously with the flow model equations.[39]

Boundary Conditions

For the simulation of fluid flow, a fixed-velocity condition is imposed at the domain inlet, and a "pressure outlet condition" is used at the outlets. Special "wall functions" are used as boundary conditions at the walls are used in order to achieve reasonable accuracy on a coarse grid.[5] The particles are assumed to escape at the top surface and the outlet, and be reflected at other walls. Recently, an accurate entrapment criterion of inclusions/small bubbles into the solidified shell was developed.[40,41] It is based on performing a sophisticated force bal-

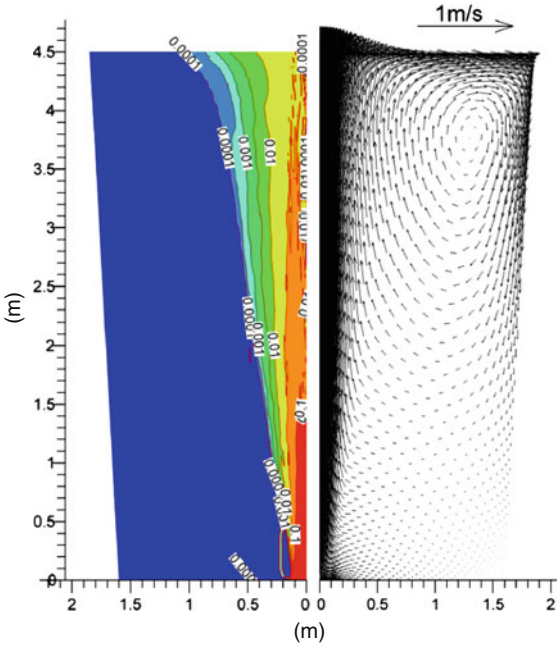

(a) Gas volume fraction and velocity vector

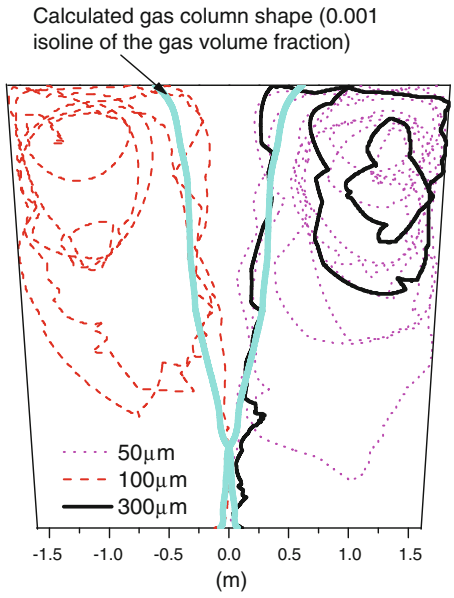

(b) Trajectories of inclusions and bubbles

Fig. 1. Fluid-flow and particle trajectories in an argon-stirred ladle.

ance on each particle and time increment in the fluid boundary layer ahead of a solidifying dendritic interface, as reported elsewhere.[40,41]

Recent Application of CFD to Steel Refining and Casting Processes

A Lagrangian–Lagrangian method has been developed using FLUENT[42] and applied to simulate

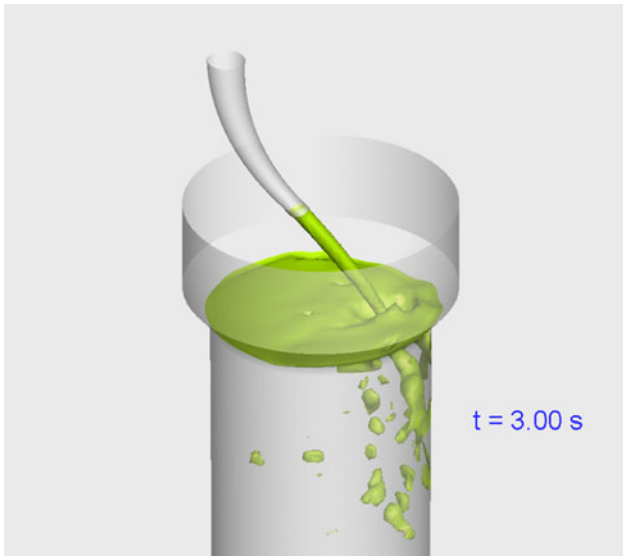

Fig. 2. The top surface fluctuation and gas entrainment in a mold during centrifugal continuous-casting process.

two-phase fluid flow in an argon-stirred 300-tonne steel ladle with 4.5 height, 0.5 Nl/min gas injection, and 30 mm bubble size.[43] The classic recirculating fluid-flow pattern is generated by argon injection from the center of the ladle bottom. Similar results were obtained in a simulation with an off-center bottom injection point.[44] The recirculating path length of inclusions in the ladle is more than 10 times that of the ladle height before they touch the top surface. The path length of the argon bubbles, however, is nearly the same as the ladle height, as shown in Fig. 1. Taking into account the initial freezing and later remelting of a solid steel shell around the alloy particles, a simulation of alloy mixing the ladle successfully matched measurements of alloy concentration with time.[44] Inclusions will be more easily removed if attached on the bubble surface. A fundamental modeling study was performed to quantify the frequency of nonwetting particle attachment to bubbles in steel as a function of particle size and bubble size.[45]

The free-surface phenomena during a centrifugal continuous-casting process were simulated using VOF multiphase model. As shown in Fig. 2, the steel jet impinges on the top surface of the mold and penetrates into the molten steel. Since the nozzle is not submerged, air is entrained into the molten steel. The motion of the air bubbles and the surface fluctuation can be well revealed, and the optimized parameters to achieve less fluctuation and less air entrainment can be obtained by the multiphase fluid-flow simulation.

PAPERS INCLUDED IN THIS *JOM* TOPIC

This section of *JOM* focuses on CFD modeling on the transport phenomena during casting to provide the state of the art in using CFD to optimize casting

operations. Lifeng Zhang and Yufeng Wang investigated the entrapment of nonmetallic inclusions in steel continuous-casting billets using CFD modeling; Hong Lei discussed the similarity of continuous-casting mold metallurgy; and Yongfeng Chen et al. studied the effect of self-braking submerged entry nozzle on steel continuous-casting operation using water modeling.

REFERENCES

1. S.V. Patankar, *Numerical Heat Transfer and Fluid Flow* (New York: McGraw Hill, 1980).
2. S.V. Patankar and B.D. Spalding, *Int. J. Heat Mass Trans.* 15, 1787 (1972).
3. B.G. Thomas, Q. Yuan, S. Sivaramakrishnan, T. Shi, S.P. Vanka, and M.B. Assar, *ISIJ Int.* 41, 1262 (2001).
4. J. Szekely and R.T. Yadoya, *Metall. Mater. Trans.* 4, 1379 (1973).
5. B.E. Launder and D.B. Spalding, *Comput. Methods Appl. Mech. Eng.* 13, 269 (1974).
6. J. Smagorinsky, *Mon. Weather Rev.* 91, 99 (1963).
7. S. Sivaramakrishnan, B.G. Thomas, and S.P. Vanka, *Materials Processing in the Computer Age*, Vol. 3, ed. V. Voller and H. Henein (Warrendale, PA: TMS, 2000), pp. 189–198.
8. Y. Tanizawa, M. Toyoda, K. Takatani, and T. Hamana, *La Revue de Metallurgie - CIT* 90, 993–1000 (1993).
9. I. Sawada, Y. Kishida, K. Okazawa, and H. Tanaka, *Tetsu-to-Hagané* 79, 160 (1993).
10. I. Sawada, K. Okazawa, E. Takeuchi, K. Shigematsu, and H. Tanaka, *Nippon Steel Tech. Report* 67, 7 (1995).
11. M. Yao, M. Ichimiya, M. Tamiya, K. Suzuki, K. Sugiyama, and R. Mesaki, *Trans. Iron Steel Inst. Jpn.* 24, s211 (1984).
12. M. Yao, M. Ichimiya, S. Kiyohara, K. Suzuki, K. Sugiyama, and R. Mesaki, *68th Steelmaking Conference Proceedings* (Warrendale, PA: ISS, 1985), pp. 27–33.
13. B.G. Thomas and F.M. Najjar, *Appl. Math. Model.* 15, 226 (1991).
14. D.E. Hershey, B.G. Thomas, and F.M. Najjar, *Int. J. Numer. Meth. Fluids* 17, 23 (1993).
15. J. Szekely and V. Stanek, *Metall. Trans.* 1, 119 (1970).
16. B. Grimm, P. Andrzejewski, K. Muller, and K.-H. Tacke, *Steel Res.* 70 (10), (1999).
17. B. Grimm, P. Andrzejewski, K. Wagner, and K.-H. Tacke, *Stahl Eisen* 115, 71 (1995).
18. R.H.M.G. Nabben, R.P.J. Duursma, A.A. Kamperman, and J.L. Lagerberg, *Ironmaking Steelmaking* 25, 403 (1998).
19. R.C. Sussman, M. Burns, X. Huang, and B.G. Thomas, *10th Process Technology Conference Proc.,* Vol. 10 (Warrendale, PA: ISS, 1992), pp. 291–304.
20. B.G. Thomas, A. Denissov, and H. Bai, *Steelmaking Conference Proceedings,* Vol. 80 (Warrendale, PA: ISS, 1997), pp. 375–384.
21. M.R. Aboutalebi, M. Hasan, and R.I.L. Guthrie, *Metall. Mater. Trans. B* 26B, 731 (1995).
22. S. Asai and J. Szekely, *Ironmaking Steelmaking* 3, 205 (1975).
23. Y. Ho, C. Chen, and W. Hwang, *ISIJ Int.* 34, 255 (1994).
24. Y. Ho and W. Hwang, *ISIJ Int.* 36, 1030 (1996).
25. L. Zhang, *Model. Simul. Mater. Sci. Eng.* 8, 463 (2000).
26. N. Bessho, R. Yoda, and H. Yamasaki, *Proc. 6th Int. Iron and Steel Congress,* Vol. 3 (Tokyo, Japan: ISIJ, 1990), pp. 340–347.
27. N. Bessho, R. Yoda, H. Yamasaki, T. Fujii, T. Nozaki, and S. Takatori, *Iron Steelmaker* 18, 39 (1991).
28. B.G. Thomas and X. Huang, *Proc. 76th Steelmaking Conference,* Vol. 76 (Warrendale, PA: Iron and Steel Society, 1993), pp. 273–289.
29. B.G. Thomas, X. Huang, and R.C. Sussman, *Metall. Trans. B* 25B, 527 (1994).
30. Y. Hwang, P. Cha, H. Nam, K. Moon, and J. Yoon, *ISIJ Int.* 37, 659 (1997).
31. L. Zhang and B.G. Thomas, *Proc. XXIV Steelmaking National Symposium Mexico* (Morelia, Mich, Mexico, 26–28 November 2003), pp. 184–198.
32. N. Kubo, J. Kubota, M. Suzuki, and T. Ishii, *Nippon Steel Tech. Report* 164, 1 (1998).
33. H. Turkoglu and B. Farouk, *ISIJ Int.* 31, 1371 (1991).
34. D. Creech (M.S. Thesis, University of Illinois at Urbana-Champaign, 1998).
35. I. Hamill and T. Lucas, *Fluid Flow Phenomena in Metals Processing*, ed. N. El-Kaddah, D.G.C. Robertson, S.T. Johansen, and V.R. Voller (Warrendale, PA: TMS, 1999), pp. 279–286.
36. Y. Sato and K. Sekoguchi, *Int. J. Multiphase Flow* 2, 79 (1975).
37. C.W. Hirt and B.D. Nichols, *J. Comput. Phys.* 39, 201 (1981).
38. O.J. Ilegbusi and J. Szekely, *ISIJ Int.* 34, 943 (1994).
39. T. Ishii, S.S. Sazhin, and M. Makhlouf, *Ironmaking Steelmaking* 23, 267 (1996).
40. Q. Yuan (Ph.D. Thesis, University of Illinois at Urbana-Champaign, 2004).
41. B.G. Thomas, L. Zhang, Q. Yuan, and S.P. Vanka, *2005 NSF Design, Manufacture and Industrial Innovation Grantees Conf. Proceedings,* ed. J. Shaw (Tempe, AZ: Arizona State University, 2005), T/BGT/1-24.
42. Fluent, Inc., *FLUENT5.1, Report* (Lebanon, NH: Fluent Inc., 2000).
43. L. Zhang, B.G. Thomas, K. Cai, L. Zhu, and J. Cui, *ISSTech2003* (Warrendale, PA: ISS, 2003), pp. 141–156.
44. J. Aoki, B.G. Thomas, J. Peter, and K.D. Peaslee, *AISTech2004* (Warrendale, PA: AIST, 2004), pp. 1045–1056.
45. J. Aoki, L. Zhang, and B.G. Thomas, *3rd Int. Congress on the Science and Technology of Steelmaking* (Warrendale, PA: AIST, 2005).